

Volume 12, Issue 2, October 2025, pp. 254-263 ISSN 2355-5068; e-ISSN 2622-4852

DOI: 10.33019/jurnalecotipe.v12i2.4575

Adaptive PID-PD Hybrid Control for Precise Motion of ROVs in Dynamic Environments

Hendi Purnata¹, Hera Susanti², Dwi Sahidin³, Galih Mustiko Aji⁴, Nanda Pranandita⁵

Mechatronics Engineering, Cilacap State of Polytechnic, Jl. Dr. Soetomo No. 1, Cilacap 53212, Indonesia
 ^{2,4}Electronics Engineering, Cilacap State of Polytechnic, Jl. Dr. Soetomo No. 1, Cilacap 53212, Indonesia
 ³Electrical Engineering, Cilacap State of Polytechnic, Jl. Dr. Soetomo No. 1, Cilacap 53212, Indonesia
 ⁵Mechanical Engineering and Manufacturing, Bangka Belitung State Polytechnic of Manufacturing, Kawasan Industri Airkantung, Sungailiat, Bangka, 33211, Indonesia

ARTICLE INFO

Article historys:

Received: 13/08/2025 Revised: 23/09/2025 Accepted: 30/10/2025

Keywords:

Dynamic Marine Conditions; Marine Robotics; PD Controller; PID Controller; Remotely Operated Vehicles; Rotation Control; ROV Position Control; Underwater Robotics

ABSTRACT

This study aims to develop and evaluate an Adaptive PID-PD Hybrid Control System to enhance the position and rotation control of a Remotely Operated Vehicle (ROV) in challenging sea conditions. In this study, two main stages were conducted. First, a dynamic model of the ROV was developed, encompassing translation for movement in three-dimensional space (x, y, z) and rotation for changes in orientation (roll, pitch, yaw). Second, the adaptive PID-PD hybrid controllers were implemented and evaluated on the ROV model to ensure stability and precision in motion control. Simulation results demonstrate that the proposed controller effectively maintains position with surge overshoot of 23.3%, sway of 1.67%, and heave of 47.17%. The settling time ranges from 41.53 to 107 seconds, indicating areas for further tuning. In terms of velocity response, surge velocity shows a high overshoot of 106.26%, while sway and heave velocities present smaller overshoots but require longer stabilization times. The integration of PID and PD in a hybrid adaptive framework yields improved inner-loop response and overall robustness. These findings highlight the potential of the adaptive hybrid controller to enhance stability, responsiveness, and operational effectiveness of ROVs in dynamic marine conditions.



This work is licensed under a Creative Commons Attribution 4.0 International License

Email: jurnalecotipe@ubb.ac.id

Corresponding Author:

Hendi Purnata

Mechatronics Engineering, Cilacap State of Polytechnic, Jl. Dr. Soetomo No. 1, Cilacap 53212, Indonesia

Email: hendipurnanta@pnc.ac.id

1. INTRODUCTION

Remotely Operated Vehicles (ROVs) have become an essential tool in the exploration and maintenance of underwater systems, such as oil drilling, marine ecosystem monitoring, and search and rescue operations [1]. With the advancement of technology and the increasing demand for operations in extreme deep-sea environments, the primary challenge in using ROVs is maintaining the stability of the vehicle's position and rotation in a dynamic marine environment. Factors such as ocean currents, waves, and pressure changes pose significant obstacles to the accurate and efficient operation of ROVs [[2], [3], [4].

Environmental constraints faced by ROVs during underwater operations include unique underwater challenges that affect positioning, navigation, and timing performance, as well as increased pressure at depth, leading to large physical systems with high operational costs [5], [6]. Technological

Volume 12, Issue 2, October 2025, pp. 254-263 ISSN 2355-5068; e-ISSN 2622-4852 **DOI:** 10.33019/jurnalecotipe.v12i2.4575

advancements in ROVs to address these challenges include the development of lighter and smaller ROVs through the use of hollow carbon fiber structural components and optical fiber microtethers, enhancing accessibility to the world's oceans. Additionally, the use of cost-effective DIY kits and adaptation to existing ROV platforms is expected to expand the reach of this technology, making ROVs more widely available [7], [8], [9]

Several studies to overcome challenges in robotic systems involve regulating motors so that they can follow the desired set point, as in the study [10], [11] sing PID controller control to regulate speed so that it matches the desired position. Then, research from [11], [12], [13] utilizing a combination of PID control and neural networks to produce an appropriate control method. However, some of the above studies have not been applied to robotic systems such as ROVs, so it is a challenge to implement the control system into robotic systems.

To address these challenges, various innovations have been developed, including the creation of lighter and more compact ROVs using materials such as hollow carbon fiber, the use of optical fiber micro-tethers, and modular systems to facilitate maintenance and mission adaptation [14], [15]. However, the greatest challenge remains in maintaining position and rotation control under the influence of dynamic marine environments. Adaptive control systems are crucial for maintaining ROV stability. One widely used method is the PID (Proportional-Integral-Derivative) controller, which can provide quick responses to disturbances, although its settings must be optimized to remain stable under extreme conditions [[16], [17], [18] The integration of PID with Proportional—Derivative (PD) control in a hybrid adaptive framework offers promising improvements in system responsiveness and robustness.

Accordingly, this study aims to develop and evaluate an Adaptive PID-PD Hybrid Control System to enhance position and orientation stability of ROVs in dynamic marine environments, thereby improving operational effectiveness and minimizing the risk of instability-induced damage during underwater missions.

2. RESEARCH METHOD

This research is an experimental study employing simulation and control system analysis, with the aim of developing and evaluating an Adaptive PID–PD Hybrid Controller to maintain the position and orientation stability of an ROV under dynamic marine conditions. The study consists of two main stages. First, a dynamic model of the ROV was developed, incorporating translational motion in three-dimensional space (x, y, z) as well as rotational dynamics for orientation changes (roll, pitch, yaw). Second, the adaptive PID–PD hybrid controllers were implemented and evaluated on the ROV model. Simulations were carried out to assess performance under environmental disturbances such as currents, waves, and hydrodynamic drag forces, with the objective of improving the ROV's stability, responsiveness, and control accuracy. The simulations were conducted using MATLAB/Simulink, which is widely used for control system analysis and simulation of dynamic models. SolidWorks was utilized for modeling the ROV geometry.

2.1. ROV Model

The ROV used in this study is equipped with eight actuators or octarotors, as shown in Figure 1. The dynamic model of the ROV can be divided into two main parts: translation equations for movement in three-dimensional space (x, y, z), and rotation equations for changes in orientation (roll, pitch, yaw).

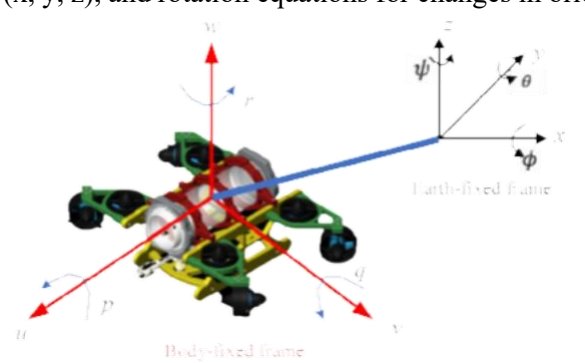


Figure 1. ROV Model Body-fixed coordinate frame and Earth-fixed coordinate frame

Volume 12, Issue 2, October 2025, pp. 254-263 ISSN 2355-5068; e-ISSN 2622-4852

DOI: 10.33019/jurnalecotipe.v12i2.4575

Figure 1 shows the geometric model of the ROV modeled by SolidWorksTM. The ROV model is powered by eight brushless DC thrusters (T1–T8) for *surge, sway, heave, roll, pitch, and yaw* movements. Mechanical properties such as mass, moment of inertia, center of gravity, and buoyancy of the ROV were obtained, with a The mass of the ROV was assumed to be 30 kg in air, with buoyancy forces calculated based on the dimensions and material properties of the ROV. The model assumes a water density of 1000 kg/m³, and the effects of ocean currents and drag forces were simulated based on typical deep-sea conditions. The initial conditions for the position and velocity of the ROV were set to zero, a weight of 392.4 N, and a buoyancy force of 615.5 N, with overall dimensions of 420 mm (length) × 596.57 mm (width) × 250 mm (height). The equations of motion for the ROV are given in equation (1).

$$M_{\mathcal{V}} + C(v) v + D(v) + G_f(\eta) = \tau \tag{1}$$

In this equation, $M_{\mathcal{V}}$ represents the inertial mass matrix, C(v) is the Coriolis matrix, and D (us the damping force matrix, while G_f is the gravitational force vector. These components describe the ROV's translational and rotational motion dynamics. the body frame and Earth in Figure 1, the position and orientation are defined in the Earth-fixed frame as shown in Equation (2). Additionally, the linear velocity and angular velocity of the ROV are presented in the body-fixed frame (2) as shown in Equation (3).

$$\eta = \left[x \, y \, z \, \phi \, \theta \, \psi \, \right] \tag{2}$$

$$v = [v w]^T = [u v w p q r]^2$$
(3)

The vector η represents the ROV's position and orientation in space, with x,y,z denoting the linear positions and φ , θ , ψ the roll, pitch, and yaw angles, respectively. The velocity in the Earth-fixed frame can be obtained from the ROV velocity in the body-fixed frame through the following transformation.

$$\dot{\eta} = J(\eta)v \tag{4}$$

The sum of the inertial mass and the fluid inertia matrix can be written as M = MRB + MA where the inertial mass of the body and the mass can be rewritten as:

$$\mathbf{M_{RB}} = \begin{bmatrix} m & 0 & 0 & 0 & mz_G & -my_G \\ 0 & m & 0 & -mz_G & 0 & mx_G \\ 0 & 0 & m & my_G & -mz_G & 0 \\ 0 & -mz_G 0 & my_G & l_x & -l_{xy} & -l_{xz} \\ mz_G & mx_G & -mx_G 0 & -l_{yx} & l_y & -l_{yz} \\ -my_G & & & -l_{xx} & -l_{zy} & l_z \end{bmatrix}$$
(5)

$$\mathbf{M}_{A} = \begin{bmatrix} X_{u} & X_{v} & X_{w} & X_{p} & X_{q} & X_{r} \\ Y_{u} & Y_{v} & Y_{w} & I_{n} & I_{d} & Y_{r} \\ Z_{u} & Z_{v} & Z_{w} & Z_{p} & Z_{q} & Z_{r} \\ K_{u} & K_{v} & K_{w} & K_{p} & K_{q} & K_{r} \\ M_{u} & M_{v} & M_{w} & M_{p} & M_{q} & M_{r} \\ N_{u} & N_{v} & N_{w} & N_{v} & N_{d} & N_{r} \end{bmatrix}$$

$$(6)$$

with $\Lambda_{*} = \frac{\P \Lambda}{\P \otimes }$ and so on hydrodynamic Damping Force Matrix.

$$D_L = -diag \{X_{\mathcal{U}}, Y_{\mathcal{V}}, Z_{\mathcal{W}}, K_{\mathcal{D}}, M_{\mathcal{Q}}, N_{\mathcal{T}}\}$$

$$\tag{7}$$

$$D_{q} = -diag \{X_{u|u|}, Y_{v|v|}, Z_{w|w|}, K_{p|p|}, M_{q|q|}, N_{r|r|}\}$$
(8)

The thrust generated by the ROV is represented by the propeller configuration matrix, **T**. The input forces and moments are calculated for six degrees of freedom (DOF). The forces and moments for the open-loop configuration are as follows:

Volume 12, Issue 2, October 2025, pp. 254-263 ISSN 2355-5068; e-ISSN 2622-4852 **DOI:** 10.33019/jurnalecotipe.v12i2.4575

 $τ_X = u_3 \cos \cos \alpha + u_4 \cos \cos \alpha + u_7 \cos \cos \alpha + u_8 \cos \cos \alpha$ $τ_Y = -u_1 \cos \cos \beta + u_2 \cos \cos \beta + u_3 \sin \sin \alpha - u_4 \sin \sin \alpha + u_7 \sin \sin \alpha - u_8$ $\sin \sin \alpha$ $τ_Z = u_1 \cos \cos \beta + u_2 \cos \cos \beta + u_5 + u_6 + u_7 + u_8$ $τ_Φ = 0.155u_1 \cos \cos \beta - 0.155u_2 \cos \cos \beta - 0.275u_5 + 0.275u_6 + 0.155u_7$ $\cos \cos \beta - 0.155u_8 \cos \beta$ $τ_Φ = 0.3945u_1 \cos \cos \beta + 0.3945u_2 \cos \cos \beta + 0.4305u_3 \cos \cos \beta + 0.4305u_4$ $\cos \cos \beta - 0.0355u_5 - 0.0355u_5 - 0.0355u_6 + 0.3945u_7 \cos \cos \beta + 0.3945u_8 \cos \beta$ $τ_Ψ = -0.3945u_1 \sin \sin \beta + 0.3945u_2 \sin \sin \beta - 0.6605u_3 \sin \sin \beta + 0.6605u_4$ $\sin \sin \beta - 0.3945u_7 \sin \sin \beta + 0.3945u_8 \sin \sin \beta$

The propulsion configuration matrix **T** based on the propulsion layout on the ROV platform is defined as follows:

$$T = \begin{bmatrix} \cos \alpha & \cos \alpha & 0 & 0 & 0 & \cos \alpha & \cos \alpha \\ -\cos \beta & \cos \beta & \sin \alpha & -\sin \alpha & 0 & 0 & \sin \alpha & -\sin \alpha \\ \cos \beta & \cos \beta & 0 & 0 & 1 & 0 & 1 & 1 \\ 0.155\cos \beta & -0.155\cos \beta & 0 & 0 & -0.275 & 0.275 & 0.155\cos \beta & -0.155\cos \beta \\ 0.3945\cos \beta & 0.3945\cos \beta & 0.4305\cos \beta & 0.4305\cos \beta & -0.0355 & -0.0355 & 0.3945\cos \beta & 0.3945\cos \beta \\ -0.3945\sin \beta & 0.3945\sin \beta & -0.6605\sin \beta & 0.6605\sin \beta & 0 & 0 & -0.3945\sin \beta & 0.3945\sin \beta \end{bmatrix}$$
(10)

2.2. PID Control System

Most existing ROV systems use a series of single-input single-output (SISO) PID controllers, where each controller is designed for one degree of freedom (DOF).

$$u = \left(k_p e(t) + K_d e(t) + K \qquad \int_0^t e(\tau) \, \mathbf{d} \right) \tag{11}$$

Where there are inner and outer PID controllers, and their gains can be adjusted or tuned according to the desired output, the following are the outer PID controller values used for six degrees of freedom (DOF). The inner and outer PID loop gains can be seen in this table:

Table 1. Adaptive PID-PD Hybrid Gain Tuning

Outer Loop (PID) - Position/Angle	Outer Kp	Outer Ki	Outer Kd	Inner Kp	Inner Kd
Surge (position)	4	0.2	2	3	0.001
Sway (position)	4	0	2	9	0.001
Heave (position)	4	0	2	10	0.001
Roll (angle)	4	0	2	10	0.001
Pitch (angle)	4	0.2	2	10	0.001
Yaw (angle)	4	0.2	2	10	0.001

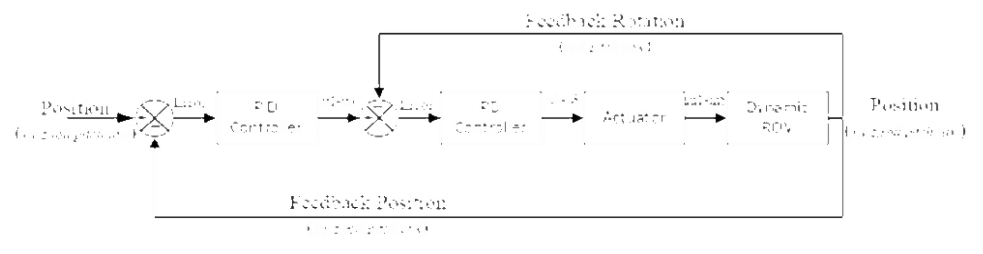


Figure 2. Adaptive PID-PD hybrid gain tuning controller block diagram of ROV

Volume 12, Issue 2, October 2025, pp. 254-263 ISSN 2355-5068 ; e-ISSN 2622-4852

DOI: 10.33019/jurnalecotipe.v12i2.4575

3. RESULTS AND DISCUSSION

In this study, an analysis was conducted on the response of the control system of an ROV operating under the influence of a dynamic marine environment. The primary objective was to evaluate the stability of the position and rotation of the ROV controlled by a Adaptive PID–PD Hybrid Gain Tuning. The simulations were performed using MATLAB/Simulink to model the dynamic ROV behavior and implement the Adaptive PID–PD Hybrid Gain Tuning. This allowed for precise control system analysis under various marine conditions. The response results showed the control system time for the 6 degrees of freedom (DOF) of the ROV: Surge, Sway, Heave, Roll, Pitch, and Yaw.

3.1. Position Response

In this study, an analysis was conducted on the surge position (x) response of the ROV with a set point depth of 5 meters. Figure 3 shows the control system response time for the surge position.

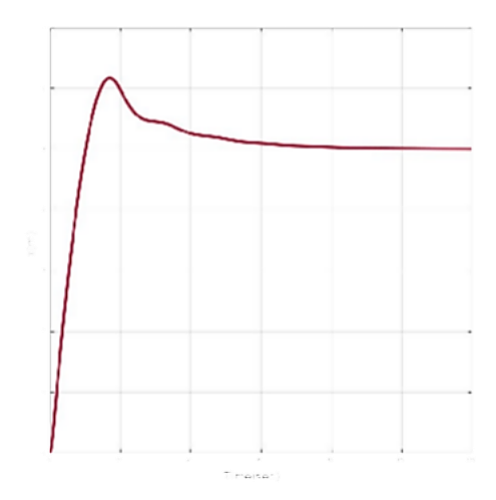


Figure 3. Surge Response (x)

For the Surge channel (x), the analysis results show that the final position reached approximately 5.006 meters, very close to the desired set point value, with an overshoot of 23.3%. This indicates that although the ROV successfully reached the target position, there was a slight excessive movement that exceeded the set point value initially. The rise time was recorded at approximately 7.59 seconds, indicating a relatively fast response toward the target position. However, the system required a settling time of approximately 57.9 seconds to stabilize at the final position. Overall, this surge response can be considered a fairly fast *step response* with some overshoot and moderate settling time, although further optimization of the PID controller is needed to reduce overshoot and accelerate stabilization time.

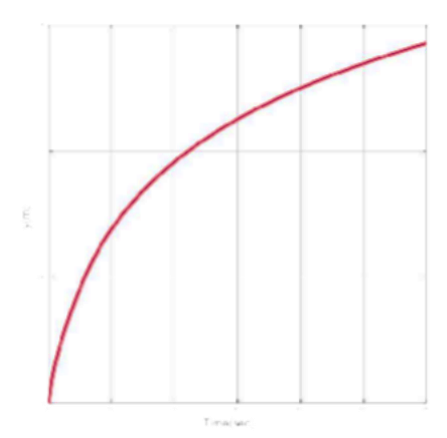


Figure 4. Sway Position

Volume 12, Issue 2, October 2025, pp. 254-263 ISSN 2355-5068 ; e-ISSN 2622-4852

DOI: 10.33019/jurnalecotipe.v12i2.4575

Figure 4 shows the Sway channel (y). The analysis results indicate that the final position is approximately 1.403 meters, very close to the desired set point. The overshoot is very small, only about 1.67%, indicating that the sway position control successfully avoided excessive movement at the beginning. However, the rise time to reach the target position is relatively slow, at approximately 80.8 seconds, indicating a slower response compared to the surge channel. Additionally, the settling time required is quite long, at 107 seconds, indicating that although the ROV eventually stabilizes at the desired position, the time required to achieve stability requires further attention.

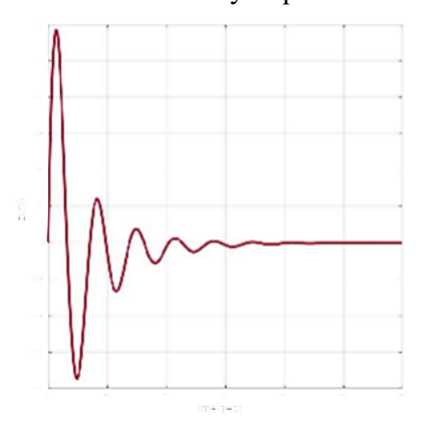


Figure 5. Heave Position

Figure 5. Shows the Heave channel (z), with the final position recorded at approximately -6.0e-5 meters, very close to zero, indicating that the system successfully returned the position to a stable value. The peak deviation was recorded at approximately 0.117 meters at 2.74 seconds, indicating initial oscillations before reaching a stable value. Following this oscillation, the settling time required was 52.3 seconds, indicating that although the system eventually stabilized at the desired value, it took a significant amount of time to come to a complete stop. Overall, this response demonstrates the presence of initial damped oscillations, which eventually settle at a stable position near zero meters, but require a prolonged stabilization period.

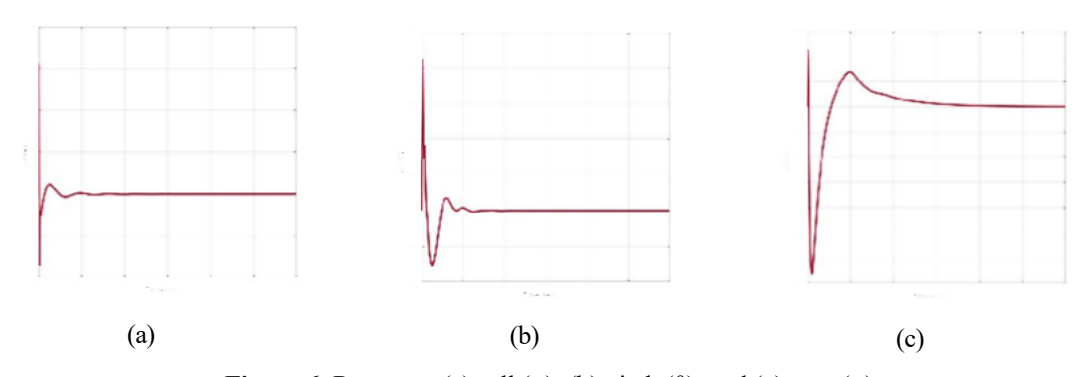


Figure 6. Response (a) roll (φ), (b) pitch (θ), and (c) yaw (ψ)

Figure 6 shows the response graph for roll (φ) , pitch (θ) , and yaw (ψ) , indicating that the control of roll and pitch successfully damped quickly to very small final values, $-3.65e-6^{\circ}$ and $-4.0e-7^{\circ}$, respectively, with relatively small peak deviations and fast settling times (approximately 13.37 seconds for roll and 15.45 seconds for pitch). This indicates that both rotation channels are sufficiently stable with short stabilization times. However, for yaw, although the final value is very small $(3.29e-5^{\circ})$, there is a larger overshoot with a peak deviation of 0.03312° at 2.16 seconds, and a much longer settling time of approximately 57.31 seconds, indicating larger initial oscillations and longer settling times. This indicates that the control settings for yaw may require further adjustment to reduce overshoot and accelerate the stabilization time.

The surge position (x) showed a final position of approximately 5.006 meters, with a 23.3% overshoot. This result, although close to the desired set point, indicates that while the ROV successfully

Volume 12, Issue 2, October 2025, pp. 254-263 ISSN 2355-5068 ; e-ISSN 2622-4852

DOI: 10.33019/jurnalecotipe.v12i2.4575

reached the target position, there was initial excessive movement. The sway position (y) demonstrated excellent stability, with only a 1.67% overshoot, though the response time was slower, with a rise time of 80.8 seconds. Heave position (z) returned to a stable value near zero after experiencing a peak deviation of 0.117 meters at 2.74 seconds, and the system required 52.3 seconds to stabilize. The roll, pitch, and yaw angles all exhibited fast stabilization times, with roll and pitch showing excellent damping, while yaw required longer settling times due to higher overshoot and initial oscillations.

3.2. Velocity Response

In this section, we will analyze the velocity response of the ROV with a desired set point for a speed of approximately 0 m/s. The figure shows the velocity response of the ROV controlled by the Adaptive PID–PD Hybrid Gain Tuning.

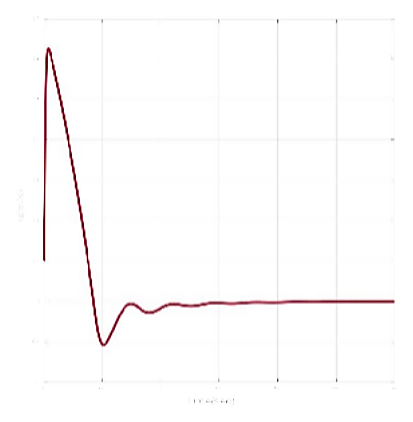


Figure 7. Surge Velocity Response

Figure 7 shows the surge velocity (u) channel, with a final value recorded at approximately -3.09e-4 m/s, indicating a slight deviation from zero. The peak deviation was recorded at approximately 0.6256 m/s at 1.56 seconds, indicating a large overshoot at the beginning. After that, the system underwent a settling process with a time of approximately 40.94 seconds, indicating that although the ROV eventually reached a more stable velocity value, the system required a considerable amount of time to fully stabilize. The rise time was recorded at approximately 1.52 seconds, indicating that the system is sufficiently responsive in reaching the final value, but with a significant overshoot (approximately 106.26%), suggesting that the PID controller settings may require further adjustment, particularly to reduce overshoot and accelerate the stabilization process.

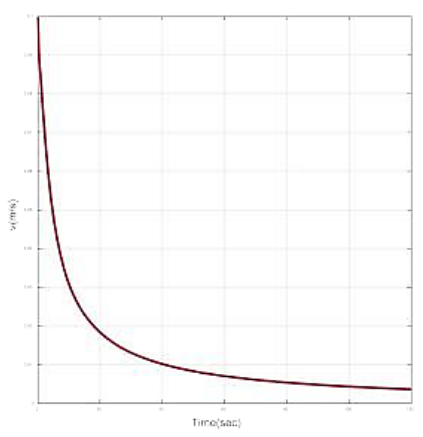


Figure 8. Sway Velocity Response

Figure 8 shows the sway velocity (v) channel, with a final value recorded at approximately 3.87e–3 m/s, with very little overshoot, only 0.20%. This indicates that although the system control has avoided excessive movement, the recorded rise time is 28.50 seconds, which is very slow. This indicates that the system requires a long time to respond and reach a stable position. Additionally, the long settling time

Volume 12, Issue 2, October 2025, pp. 254-263 ISSN 2355-5068 ; e-ISSN 2622-4852 **DOI:** 10.33019/jurnalecotipe.v12i2.4575

(74.51 seconds) indicates significant drift in the sway position, which may be caused by insufficiently aggressive inner-loop tuning or asymmetry in the drag forces. Overall, this sway response requires an increase in inner-loop gain to accelerate response time and reduce the drift occurring.

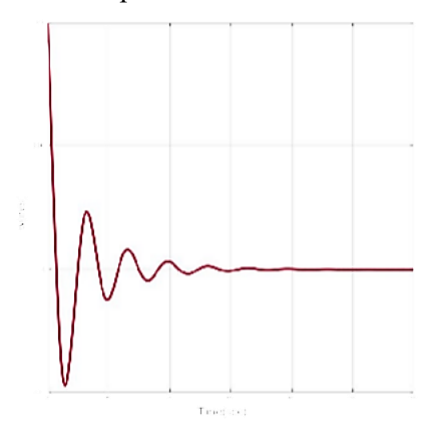


Figure 9. Heave Velocity Response

Figure 9. This is the heave velocity (w) channel, with a final value recorded at approximately 4.19e-7 m/s, which is very close to zero, indicating that the control system successfully returned the position to a stable state near zero. The overshoot is 47.17% smaller than the surge, but still indicates excessive movement before finally stabilizing. The rise time is recorded at 2.21 seconds, which is faster than some other channels, indicating that the system can respond quickly. However, the relatively long settling time (41.53 seconds) indicates that although the heave was successfully stabilized, the stabilization process took longer. This suggests that while the rise time control is adequate, the PID settings in the inner loop need to be adjusted to accelerate the stabilization process without compromising stability.

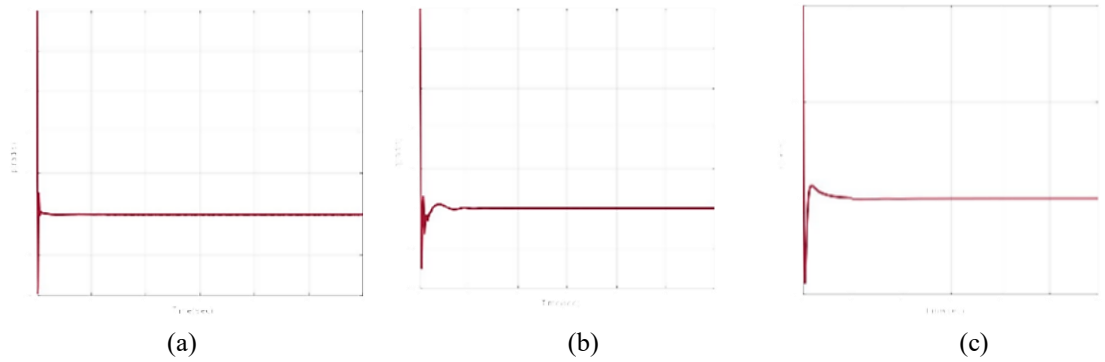


Figure 10. Roll rate (p), Pitch rate (q), and Yaw rate (r) response

Figure 10 shows the analysis of roll rate (p), pitch rate (q), and yaw rate (r). The graph indicates that the roll rate can return to a stable position very quickly, with a final value recorded at -1.70e-5 deg/s. The overshoot in the roll rate of 39.29% indicates an initial swing, but the very fast rise time (0.078 seconds) and settling time of only 0.98 seconds show that the system responds very well and stabilizes quickly. For the pitch rate, the final value is very small (3.04e-9 deg/s), but the overshoot is higher (30.09%) and the settling time is longer (8.87 seconds), indicating a slightly slower response and requiring more time to stabilize. For yaw rate, although the rise time is fast (0.199 seconds), the overshoot is 43.87% and the settling time is quite long (9.75 seconds), indicating a large initial swing and a longer stabilization time.

The analysis of velocity responses revealed similar trends. Surge velocity experienced a large overshoot (106.26%), highlighting the need for further optimization in the inner-loop control. On the other hand, the sway velocity showed minimal overshoot (0.20%) but exhibited slower stabilization, taking 74.51 seconds to reach a stable value. Heave velocity had a 47.17% overshoot, with the system

Volume 12, Issue 2, October 2025, pp. 254-263 ISSN 2355-5068; e-ISSN 2622-4852

DOI: 10.33019/jurnalecotipe.v12i2.4575

requiring 41.53 seconds for stabilization, suggesting that adjustments to the PID settings are needed for faster stabilization.

Overall, the roll rate demonstrates highly responsive and stable control, with moderate overshoot and very fast settling time. The pitch rate has slightly higher overshoot and requires a longer stabilization time, while the yaw rate shows significant overshoot and the longest settling time. This indicates that for the yaw rate, control settings need to be adjusted to reduce overshoot and accelerate the stabilization process, while for roll and pitch, control settings are already adequate although slight adjustments to the gain are needed to speed up the response.

4. CONCLUSION

This study successfully developed and evaluated an Adaptive PID-PD Hybrid Controller to improve the position and rotation control of a Remotely Operated Vehicle (ROV) in a dynamic marine environment. Simulation results showed that the Cascade PID controller successfully maintained the ROV's position with surge overshoot reaching 23.3%, sway only 1.67%, and heave around 47.17%. The settling time required for stabilization ranged from 41.53 to 107 seconds, with rise times varying from 1.52 seconds (surge velocity) to 28.50 seconds (sway velocity). In terms of velocity, the surge velocity experienced a large overshoot of 106.26%, while the sway velocity and heave velocity had smaller overshoots with longer stabilization times. Overall, the adaptive PID-PD hybrid framework proved effective in maintaining the stability of the ROV's position and rotation; however, further optimization of the inner-loop gain is required to reduce overshoot and accelerate stabilization time, particularly in the sway and yaw channels. Additional adjustments to the PID gain are expected to enhance system responsiveness, reduce drift, and improve the ROV's speed and position stabilization in dynamic sea conditions. Moving forward, future research should explore adaptive control to enable real-time adjustments to system parameters based on changing environmental conditions, such as fluctuating currents and wave heights. Additionally, integrating machine learning could allow ROVs to autonomously optimize control parameters, making them more resilient and responsive in dynamic conditions. These advancements would position this study as a significant step forward in autonomous underwater systems and pave the way for further innovations in marine robotics.

Acknowledgments

This research was supported by the Research and Community Service Center (P3M) of the Cilacap State Polytechnic and DPPM Kemendiktisaintek. We would like to thank all those who have provided support and contributed to the implementation of this research. The support we received was very meaningful in realizing the technological development that we are studying.

REFERENCES

- [1] Y. Chen, H. Zhang, W. Zou, H. Zhang, B. Zhou, and D. Xu, "Dynamic modeling and learning based path tracking control for ROV-based deep-sea mining vehicle," *Expert Syst. Appl.*, vol. 262, p. 125612, 2024, https://doi.org/10.1016/j.eswa.2024.125612
- [2] Tran, N.-H., Le, M.-C., Ton, T., Le, T.-C., & Tran, T. (2020). ROV Stabilization Using an Adaptive Nonlinear Feedback Controller. In *Lecture Notes in Computer Science*, 144–155. https://doi.org/10.1007/978-3-030-62324-1_13.
- [3] Sahili, J., Hamoud, A., & Jammoul, A. (2018). ROV Design Optimization: Effect on Stability and Drag Force. In 2018 6th RSI International Conference on Robotics and Mechatronics (IcRoM), 413–417. https://doi.org/10.1109/ICROM.2018.8657510
- [4] Yang, Y., Yang, R., Qin, H., Li, R., & Ye, W. (2024). Research on Vision-Based ROV Underwater Positioning Method. In *Proceedings of the 2024 5th International Conference on Geology, Mapping, and Remote Sensing (ICGMRS)*, 131–137. https://doi.org/10.1109/ICGMRS62107.2024.10581261
- [5] Diamanti, E., Mentogiannis, V., Ødegård, Ø., & Koutsouflakis, G. (2025). Underwater drones as



Volume 12, Issue 2, October 2025, pp. 254-263 ISSN 2355-5068; e-ISSN 2622-4852 **DOI:** 10.33019/jurnalecotipe.v12i2.4575

- a low-cost, yet powerful tool for underwater archaeological mapping: Case studies from the Mediterranean. *Journal of Computer Applications in Archaeology*, 8(1), 10–24. https://doi.org/10.5334/jcaa.184
- [6] Salah, S., et al. (2021). Design of lightweight, low-cost remotely operated underwater vehicle. In *Proceedings of the ASME Design Engineering Technical Conference*. https://doi.org/10.1115/DETC2021-70555.
- [7] McCulley, R. (2009). Almost disposable ROVs earning respect offshore. *Offshore Engineer*, 34(5). Retrieved from https://www.scopus.com/inward/record.uri?eid=2-s2.0-67650723276&partnerID=40&md5=74848ea67f12dfc35ffe54ce9c7dae59
- [8] Poretti, M., Benson, B., & Rauch, C. (2013). Design of modular camera tool for mini underwater ROVs. In *OCEANS 2013 MTS/IEEE San Diego: An Ocean in Common*. https://www.scopus.com/inward/record.uri?eid=2-s2.0-84896368489&partnerID=40&md5=448b0974ee92f9e06c8ba20cd8641d6a
- [9] Ravichandran, S., et al. (2022). Accelerated testing and results of underwater electric thrusters for mini observation class ROVs. In *Oceans Conference Record (IEEE)*. https://doi.org/10.1109/OCEANSChennai45887.2022.9775357.
- [10] Mansoor, A., Salih, T., & Abdullah, F. (2022). Speed Control of Separately Excited D.C. Motor using Self-Tuned Parameters of PID Controller. *Tikrit Journal of Engineering Sciences*, 20(1), 1–8. https://doi.org/10.25130/tjes.20.1.01.
- [11] Wu, X.-G., Wang, X.-D., Yu, T.-W., & Xie, X.-P. (2007). PID control on the current of electromagnetic clutch tuned by neural network. *Dianji yu Kongzhi Xuebao/Electric Machines and Control*, 11(4), 335–339. https://www.scopus.com/inward/record.uri?eid=2-s2.0-34547976761&partnerID=40&md5=b16f8f07ba1451e7972865fb176f4e5e
- [12] Li, J., Zhang, L., Huang, X., Zhang, Q., & Wang, G. (2022). Cascade PID control algorithm for wind turbine blade mold temperature based on improved RBF neural network. *Taiyangneng Xuebao/Acta Energiae Solaris Sinica*, 43(3), 330–335. https://doi.org/10.19912/j.0254-0096.tynxb.2020-0640.
- [13] He, D., Shi, F., Tan, S., & Deng, Q. (2020). Research on inverse kinematics algorithm of 6-DOF industrial robot based on RBF-PID. *Journal of Physics: Conference Series*, 1624, 042017. https://doi.org/10.1088/1742-6596/1624/4/042017.
- [14] Qafko, T., et al. (2024). Design and control of an underwater remotely operated vehicle using thrust force vectors. In *URTC 2024 2024 IEEE MIT Undergraduate Research Technology Conference*, Proceedings. https://doi.org/10.1109/URTC65039.2024.10937653.
- [15] Ali, F. A., Aras, M. S. M., Azis, F. A., Sulaima, M. F., & Jaaffar, I. (2014). Design and development of auto depth control of Remotely Operated Vehicle using thruster system. *Journal of Mechanical Engineering and Sciences*, 7(1), 1141–1149. https://doi.org/10.15282/jmes.7.2014.13.0111.
- [16] Jayasundere, N. D., & Gunawickrama, S. (2016). Underwater ROV with fuzzy logic motion control. In 2016 IEEE International Conference on Information and Automation for Sustainability (ICIAfS), 1–6. https://doi.org/10.1109/ICIAFS.2016.7946564.
- [17] Xia, P., Zhou, T., Ye, Y., & Du, J. (2024). Human autonomy teaming for ROV shared control. *Journal of Computing in Civil Engineering*, 38, CPENG-5756. https://doi.org/10.1061/jccee5.cpeng-5756.
- [18] Tan, Y. H., Liu, X., & Chen, B. M. (2018). Hardware adaptation of a small commercial ROV for autonomous use. In 2017 Asian Control Conference, ASCC 2017, 1252–1257. https://doi.org/10.1109/ASCC.2017.8287350.